Journal of Applied Polymer Science

A novel mono-methacryloyloxy terminated fluorinated macromonomer used for the modification of UV curable acrylic copolymers

Jianquan Tan,[1,2,3] Weiqu Liu,[1,2] Honglei Wang,[1,2,3] Yang Sun,[1,2,3] Shijian Wang[1,2,3]

[1]Guangzhou Institute of Chemistry, Chinese Academy of Sciences, Guangzhou, China

[2]Key Laboratory of Cellulose and Lignocellulosics Chemistry, Chinese Academy of Sciences, Guangzhou, China

[3]University of Chinese Academy of Sciences, Beijing, China

Correspondence to: W. Liu; (E-mail: liuwq@gic.ac.cn)

ABSTRACT: A novel macromonomer containing fluorinated units (PHFBMA-GMA) was synthesized through a two-step procedure: firstly, hexafluoro-butyl methacrylate (HFBMA) was polymerized in the presence of functional chain transfer agent 3-mercaptopropionic acid (MPA) and then the carboxyl acid group terminated polymer was end-capped with glycidyl methacrylate (GMA). Chemical structures of PHFBMA-GMA were characterized by gel permeation chromatography, fourier transform infrared spectroscopy (FTIR), and ^{1}H nuclear magnetic resonance (NMR). Subsequently, PHFBMA-GMA was employed as reactive surface additives added into UV-cured polyacrylate to modify UV-curable coatings. It is convenient to control the tail length of the fluorinated segments in this study by adjusting the ratio of initiator and chain transfer agent. The influence of both the concentration and the molecular weight of PHFBMA-GMA on the surface properties of UV-cured films was investigated. With increasing both the concentration and the molecular weight of PHFBMA-GMA, the surface energy of the UV-cured films decreased. X-ray photoelectron spectroscopy was employed to characterize and quantify the surface composition and the results confirm the enrichment of fluorinate atoms on the surface. Moreover, the physical properties of UV-cured films, such as gel content, water absorption, pencil hardness, adhesion, chemical resistance, mechanical properties, optical transmittance, and thermal properties, were also investigated in detail. The novel macromonomer was economical but effective to modify the properties of the UV-curable coatings. © 2015 Wiley Periodicals, Inc. J. Appl. Polym. Sci. **2016**, *133*, 43116.

KEYWORDS: blends; coatings; functionalization of polymers; photopolymerization; surfaces and interfaces

Received 2 August 2015; accepted 2 November 2015

DOI: 10.1002/app.43116

INTRODUCTION

In the recent years, UV-cure technology is growing rapidly and has been widely used in coating industry for its low energy consumption, rapid curing process, and moderate curing conditions. UV-curable coatings have been extensively studied for optical applications, especially for organic optical resins which possess unparalleled properties such as low density, excellent transparency, and easy to process, compared to glass.[1,2] Among UV curing coatings, UV-curable polyacrylate is one of the most widely used components for free-radical type UV-cure coating systems due to their suitability to be shaped in various molecular structures with different properties, as well as their relatively low cost.[1,3] However, some disadvantages of polyacrylate, such as low thermal resistance and high surface energy, need to be improved for further applications.

Fluoropolymers are playing an important role in coating applications due to their distinct advantages such as low surface tension, outstanding oil and water repellency, nonadhesive nature, and antifouling properties as well as their excellent thermal and chemical stability under harsh conditions.[3–10]

Copolymerization and blending are two main methods to prepare fluorinated polyacrylate materials which combine the advantages of fluoropolymer and polyacrylate. Among copolymerization method, random copolymerization of various fluorine-containing vinyl monomer and/or fluorinated acrylates is the most common one. However, in order to achieve desirable surface property, it is necessary to use a great deal of fluorinated monomers because a considerable part of fluorinated moieties are buried in the bulk of the coatings and cannot migrate to the air interface.[11] That must be not economical since most fluorinated monomers are quite expensive.

Researchers have found that long perfluoroalkyl groups have greater driving force to migrate, resulting in large amount of CF_3 groups assemble and aggregate at the polymer-air surface.[4,11–15] As a result, block copolymers with long fluorinated segments have been synthesized and investigated. On the

Table I. Reaction Formulation of UVPA Oligomer and UVSFPA Oligomer

Samples	MMA (g)	IBA (g)	AA (g)	HFBMA (g)	AIBN (g)	IOMP (g)
UVPA[a] oligomer	9.00	9.00	2.00	–	0.30	0.20
UVSFPA-2 oligomer	8.80	8.80	2.00	0.40	0.30	0.20
UVSFPA-4 oligomer	8.60	8.60	2.00	0.80	0.30	0.20
UVSFPA-6 oligomer	8.40	8.40	2.00	1.20	0.30	0.20
UVSFPA-8 oligomer	8.20	8.20	2.00	1.60	0.30	0.20
UVSFPA-10 oligomer	8.00	8.00	2.00	2.00	0.30	0.20

[a] Mn was 7546 and PDI was 2.23, data from GPC measurement.
The denotation of UVSFPA-X oligomer was employed to describe different UVSFPA oligomer samples, X represents the weight percentage of HFBMA based on the weight of the total monomers.

premise of obtaining desirable surface properties, although the usage of fluorine-containing vinyl monomer could be lowered dramatically, the synthetic methods to prepare block copolymers, such as living radical polymerization, anionic polymerization, and group transfer polymerization, are quite harsh.

In contrast with the copolymerization method, blending is a much more economical but effective method. Considering that the efficiency of fluorine could be maximized by anchoring the fluorinated group at the end of the molecular chain,[16] especially using fluoropolymer with long tail-like fluorinated segments.

Longer perfluoroalkyl chains have greater driving force to migrate to the outmost layer. Extending the length of perfluoroalkyl chains is a common method to obtain long tail-like fluorinated segments. Ameduri *et al.*[17] synthesized a series of fluorinated acrylates with various perfluoroalkyl chain length in a three-step procedure and investigated the effect of structural parameters on the surface properties of cured films. The results showed that comonomers with longer fluorinated chain length were more efficient to lower the surface energy under the same fluorine concentration. However, monomers with long perfluoroalkyl chains were not only expensive but also difficult to synthesize. While the tail length of the fluorinated segments in this study was easy to control by just adjusting the ratio of initiator and chain transfer agent. Furthermore, there are few reports concerning the preparation of reactive additive with long tail-like fluorinated segments by conventional radical polymerization.

Considering the points mentioned above, in this work, a novel macromonomer[18–20] containing fluorinated units (PHFBMA-GMA) was synthesized via thiol-ene addition.[21,22] It is convenient to control the tail length of the fluorinated segments in this study by adjusting the ratio of initiator and chain transfer agent. Then, it was used as a reactive surface additive to copolymerize with homemade acrylate UV oligomer (naming UVPA oligomer) to prepare transparent antifouling UV-cured coatings (naming UVLFPA) under UV radiation. The specifically designed fluorinated macromonomer could firmly anchor into the cross-linking network due to the methacryloyloxy at the end of the macromonomer. In addition, the long tail-like fluorinated segments have strong tendency to migrate and concentrate on the outermost layer. A series of newly fluorinated macromonomer with various molecular weights were prepared in the following procedures. Firstly, a mono-carboxyl functional poly(hexafluoro-butyl methacrylate) (PHFBMA-COOH) was prepared via radical polymerization of hexafluoro-butyl methacrylate (HFBMA) using 3-mercaptopropionic acid (MPA) as functional chain transfer agent. Then the mono-carboxyl functional PHFBMA-COOH was endcapped with glycidyl methacrylate (GMA) to produce the PHFBMA-GMA. The chemical structure of the obtained PHFBMA-GMA was characterized by gel permeation chromatography (GPC), FTIR, and ^{1}H NMR. In comparison, a series of UV-curable polyacrylate coatings prepared with short fluorinated groups (naming UVSFPA) was prepared. Contact angle measurements and surface energy were used to assess the wettability of the resulting acrylic UV-cured coatings and the surface composition was evaluated by X-ray photoelectron spectroscopy (XPS). In addition, gel content, water absorption, pencil hardness, adhesion, chemical resistance, mechanical properties, optical transmittance, and thermal properties were also investigated in detail. This study might open up an economical but effective route to prepare monomethacryloyloxy terminated reactive additives with long fluorinated chain length using in UV-curable coatings.

EXPERIMENTAL

Materials

HFBMA was purchased from Harbin Xeogia Fluorine-Silicon Chemical Co., China. Azobisisobutyronitrile (AIBN), 2,6-Di-tert-butyl-4-methylphenol (BHT), 1,4-dioxane (DO), petroleum ether, and triethylamine (TEA) were purchased from Tianjin Fuchen chemical reagents factory. MPA, isooctyl 3-mercaptopropionate (IOMP), methyl methacrylate (MMA), isobutyl acrylate (IBA), acrylic acid (AA), and GMA were purchased from Aladdin Chemistry Co., China. Tetrabutylammonium bromide (TBAB) was obtained from Tianjin Kemiou Chemical Reagent Co.. Benzophenone (BP) was obtained from Shanghai Lingfeng Chemical Reagents Co.. Pentaerythritol triacrylate (PETA) was obtained from Energy Chemical. All the materials were used as received except for AIBN which was purified by recrystallization from absolute ethyl alcohol.

Synthesis of UVPA Oligomer and UVSFPA Oligomer

The reaction formulation of UVPA oligomer and UVSFPA oligomer was summarized in Table I. Solution of appropriate amount of MMA, IBA, AA, HFBMA, AIBN, IOMP, and DO (the same weight of the unsaturated monomers) was added dropwisely into the a flask containing DO (the same weight of

Table II. Reaction Formulation and Molecular Weight of PHFBMA-GMA

Samples	HFBMA (g)	AIBN (g)	MPA (g)	GMA (g)	Mn[a]	Mn[b]	Mn[c]	PDI
PHFBMA-GMA-1/3	20.00	0.20	0.60	1.61	5257	5090	5793	1.52
PHFBMA-GMA-1/6	20.00	0.20	1.20	3.22	3285	3078	3369	1.38

[a] Mn from GPC.
[b] Mn of PHFBMA-COOH from end group titration.
[c] Mn from NMR.
The denotation of PHFBMA-GMA-X/Y was employed to describe different PHFBMA-GMA samples with various molecular weight, *X* and *Y* indicated the weight percentage of AIBN and MPA based on the weight of HFBMA, respectively.

the unsaturated monomers) under nitrogen atmosphere for 3 h. After added, the polymerization was carried out at 80°C for another 8 h, and then at 90°C for 16 h. Subsequently, GMA (0.625/1 molar ratio of GMA and AA) was added dropwisely into the solution during 1 h after TBAB (0.8 wt % of the total momoners) and BHT (0.4 wt % of the total momoners) were added. The solution was kept at 102°C for another 4 h after added.

The obtained polymer solution was added into 10 times the weight of petroleum ether and the precipitate was collected. Subsequently, the precipitate was dissolved into MEK and then precipitated in petroleum ether again. After the precipitation–dissolution process was done for five times, the collected precipitate was dried at 60°C for 24 h under vacuum condition. Yield: 90.2% for UVPA oligomer, 89.4% for UVSFPA-2 oligomer, 91.1% for UVSFPA-4 oligomer, 90.7% for UVSFPA-6 oligomer, 91.0% for UVSFPA-8 oligomer, and 89.9% for UVSFPA-10 oligomer.

Synthesis of PHFBMA-GMA

The reaction formulation of PHFBMA-GMA is summarized in Table II. Solution of appropriate amount of HFBMA, AIBN, MPA, and DO (the same weight of HFBMA) was added dropwisely during 3 h into a three-neck flask, containing DO (the same weight of HFBMA), immersed in an oil bath at 80°C under nitrogen atmosphere. After added, the system was kept at 80°C for 8 h and then at 90°C for 16 h. Subsequently, the system was heated to 102°C. GMA (2/1 molar ratio of GMA and MPA) was added dropwisely into the solution during 1 h after TBAB (0.8 wt % of HFBMA) and BHT (0.4 wt % of HFBMA) were added. The solution was kept at 102°C for another 4 h after added. The purification procedure was as follows. The obtained polymer solution was added into 10 times the weight of petroleum ether and the precipitate was collected. Subsequently, the precipitate was dissolved into DO and then precipitated in petroleum ether again. After the precipitation–dissolution process was done for five times, the collected precipitate was dried at 60°C for 24 h under vacuum condition. Yield: 82.4% for PHFBMA-GMA-1/3 and 77.8% for PHFBMA-GMA-1/6.

Preparation UV-Cured Films

UVPA was a UV-cured product blending with UVPA oligomer, PETA, and BP. It is a blank sample that without fluorine. UVSFPA was a UV-cured product blending with UVSFPA oligomer, PETA and BP. It is a sample with short fluorinated groups. UVLFPA was a UV-cured product blending with UVPA oligomer, PHFBMA-GMA, PETA, and BP. It is a sample with long tail-like fluorinated chains.

The weight composition of UVLFPA formulations is shown in Table III. Appropriate amount of PHFBMA-GMA was added into UVPA and PETA to prepare a UV-curable viscous mixture. For the UV-cured films prepared by UVPA oligomer and UVSFPA oligomer, the weight composition was UVSFPA oligomer (12.67 g), PETA (6.33 g), BP (1.00 g). For the UV-cured blank sample (naming UVPA), the weight composition

Table III. The Weight Composition of UVLFPA Formulations

Samples	UVPA oligomer (g)	PHFBMA-GMA-1/3 (g)	PHFBMA-GMA-1/6 (g)	PETA (g)	BP (g)
UVLFPA-1/3-2	12.40	0.40	-	6.20	1.00
UVLFPA-1/3-4	12.14	0.80	-	6.06	1.00
UVLFPA-1/3-6	11.87	1.20	-	5.93	1.00
UVLFPA-1/3-8	11.60	1.60	-	5.80	1.00
UVLFPA-1/3-10	11.34	2.00	-	5.66	1.00
UVLFPA-1/6-2	12.40	-	0.40	6.20	1.00
UVLFPA-1/6-4	12.14	-	0.80	6.06	1.00
UVLFPA-1/6-6	11.87	-	1.20	5.93	1.00
UVLFPA-1/6-8	11.60	-	1.60	5.80	1.00
UVLFPA-1/6-10	11.34	-	2.00	5.66	1.00

In the denotation of UVLFPA-X/Y-Z, the meaning of X/Y represents the type of PHFBMA-GMA(1/3 for PHFBMA-GMA-1/3 and 1/6 for PHFBMA-GMA-1/6, respectively), Z indicated the weight percentage of the PHFBMA-GMA macromonomer in UVLFPA.

was UVPA oligomer (12.67 g), PETA (6.33 g), and BP (1.00 g). Then the mixture was casted onto various substrates with and dried at 50°C for 24 h and then heated overnight in an oven at 50°C under vacuum to remove all solvent. Subsequently, the coated films were irradiated by a high-pressure mercury lamp (500 W) for 120 s with a distance of 20 cm from lamp to the surface of samples in air atmosphere. The film thickness is around 100 μm.

Freestanding films were prepared by pouring the UV-curable viscous mixture into a TeflonTM mold (10 mm × 75 mm × 1 mm). Mixture in the mold was covered by transparent thin polyester film in order to prevent the inhibiting effect of oxygen, a glass plate was placed over the polyester film used to obtain homogenous thickness. Finally, the formulations were irradiated by a high-pressure mercury lamp (500 W) for 600 s.

Characterization

The molecular weight distributions of the polymer samples were measured at 30°C by GPC on a Waters 2410 instrument with THF as the solvent (1.0 mL/min) and polystyrene as the calibration standards.

The FTIR spectra were obtained using a TENSOR27 (Bruker, Germany) spectrometer over the range 400–4000 cm^{-1}.

^{1}H NMR was performed on a 400-MHz Bruker NMR spectrometer using $CDCl_3$ as solvent and tetramethylsilane as an internal reference. Chemical shifts of the ^{1}H NMR were related to the $CDCl_3$ signal at 7.24 ppm.

The contact angle of water was measured on the air-side surface of the coating films with a contact goniometer (Shanghai Zhongchen, China) by the sessile drop method with a microsyringe at 25°C. The average contact angle of each sample was measured more than five times at different locations. In this study. The surface free energy was calculated by means of geometric-mean equation which was described by Owens and Wendt.[23] According to Owens and Wendt, the surface energy of a given solid can be determined using an equation applied to two liquids.

$$(1+\cos\theta)\gamma_l = 2\left(\gamma_s^{d}\gamma_l^{d}\right)^{1/2} + 2\left(\gamma_s^{nd}\gamma_l^{nd}\right)^{1/2}$$

where γ_s and γ_l are the surface free energies of the solid and pure liquid, respectively. The superscripts "d" and "nd" represent the dispersive and nondispersive contributions to the total surface energy, respectively. Water ($\gamma_l = 72.8$ mJ/m^2, $\gamma_l^{d} = 21.8$ mJ/m^2, $\gamma_l^{nd} = 51$ mJ/m^2), diiodomethane ($\gamma_l = 50.8$ mJ/m^2, $\gamma_l^{d} = 48.5$ mJ/m^2, $\gamma_l^{nd} = 2.3$ mJ/m^2).

The adhesion and the pencil hardness of the films were performed in accordance with ASTM 3359 and ASTM 3363, respectively. Sample preparation is the same as the one described in contact angle measurement.

The gel content was performed with the following procedure. The UV-cured films were extracted with acetone for 24 h. After extraction, the UV-cured films were dried in a vacuum oven until constant weight. The equation summarized below: gel content % = Wt/W_0 × 100%, where W_0 is the weight of the UV-cured film before extraction And W_t is the final weight after extraction.

Mechanical properties of the films were determined by standard tensile stress–strain tests. Stress–strain measurements were carried out at room temperature by using an universal testing machine (Reger, extension rate of 5 mm/min).

Optical transmittance characterization was conducted on a UV-2550 UV−visible spectrophotometer.

Differential scanning calorimetry (DSC) measurements were performed on DSC 204 (NETZSCH Germany) under N_2 atmosphere. Each sample (about 10 mg) was scanned from −30°C to 200°C at a heating rate of 20°C/min and held at 200°C for 5 min to remove the thermal history. Glass transition temperature (T_g) values were recorded during the second heating scan taken as the midpoint of the heat capacity change.

Thermogravimetric analysis (TGA, TG209F3 NETZSCH Germany) was performed on a TG209F3 to study the thermal stability of fluorinated UV-cured films under N_2 atmosphere. Each sample was about 5 mg and heated at the heating rate of 10°C/min from 30°C to 800°C.

RESULTS AND DISCUSSION

Synthesis and Characterization of PHFBMA-GMA and UVPA

The molecular weight of the functional macromonomer can be adjusted by changing the ratio of chain transfer agent to initiator.[24] In the present work, two types of macromonomer methacryloyloxy terminated fluorinated macromonomer were synthesized by changing the ratio of MPA to AIBN. The synthetic routes of UVPA oligomer and UVSFPA oligomer, PHFBMA-GMA, are described in Scheme 1 and Scheme 2, respectively. The GPC curves of UVPA oligomer, PHFBMA-GMA-1/3, and PHFBMA-GMA-1/6 are summarized in Figure 1. The molecular weight and molecular weight distribution were summarized in Tables I and II, respectively. As expected, the molecular weight of the macromonomer increased with the decreasing ratio of MPA to AIBN and the molecular distribution of the macromonomer is narrow.

Furthermore, the functionality is another crucial parameter to determine the structure of the macromonomer. In this article, end group titration,[25,26] GPC and ^{1}H NMR were employed to determine the functionality of PHFBMA-GMA (see Table IV). The methacryloyloxy group content of macromonomer can be calculated by the integral ratio of the protons(–C***H*****$_2$**=C(CH$_3$)–COO–, 6.05 ppm and 5.64 ppm) of the double bond in methacryloyloxy to methane proton of –CHF– (5.06–4.78 ppm).The results show that the number-average molecular weight determined by end-group titration were well consistent with the molecular weight measured by GPC and ^{1}H NMR, indicating that every PHFBMA-MPA chain contained one carboxyl acid group. Since mercapto compounds have particularly large chain transfer constant due to the weak S–H bond, the functionality of the macromonomer can be over 90% in most cases.[24–29] The results are in fair agreement with the articles.[24–29]

The chemical structures of PHFBMA-GMA and UVPA were characterized by FTIR and ^{1}H NMR spectra. Figure 2 shows the

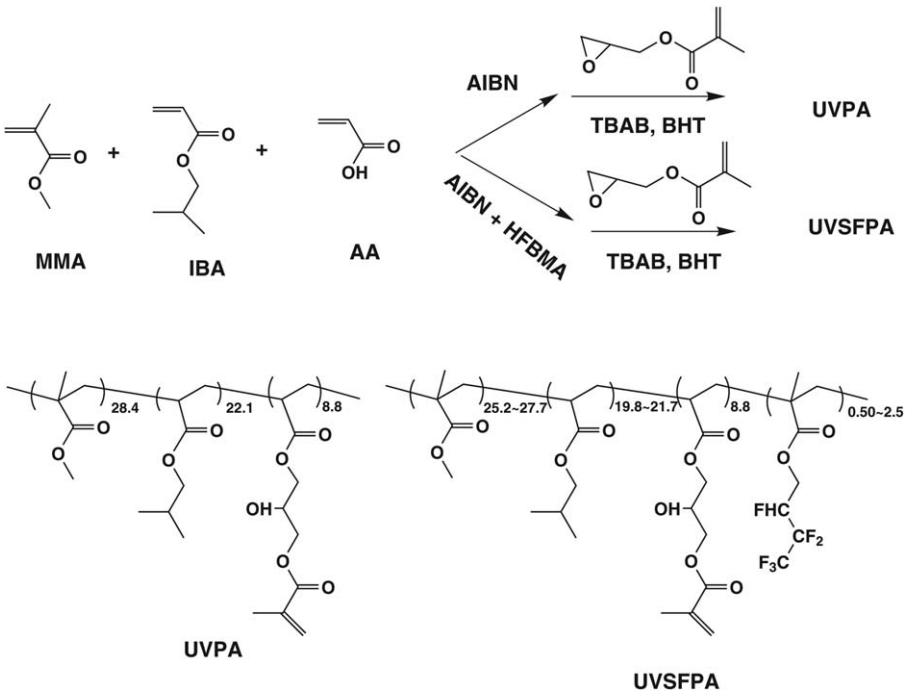

Scheme 1. Synthetic route of UVPA oligomer and UVSFPA oligomer.

FTIR spectra of UVPA oligomer (trace 1) and PHFBMA-GMA-1/6 (trace 2). In trace 1, peaks ranging from 3112 to 3707 cm^{-1} are ascribed to the absorption of OH. The signals in the range 2810–3070 cm^{-1} are assigned to the C–H stretching vibration. Peaks at 1729 cm^{-1} represented the presence of C=O stretching. Absorption at 1635 cm^{-1} represented the C=C stretching was clearly observed. No absorption at 914 cm^{-1} representing the epoxy group was detected, suggesting the completed reaction between epoxy group and carboxyl acid group.

In trace 2, the wide and dispersive absorption peak in the range 3175–3700 cm^{-1} confirmed the presence of OH in the polymer. The absorbance ranging from 2829 to 3072 cm^{-1} are ascribed to the C–H stretching's. Absorbance at 1729 cm^{-1} confirm the presence of C=O stretching and peaks at 1635 cm^{-1} are assigned to the C=C stretching vibration. Characteristic peaks at 1300 cm^{-1} and 1190 cm^{-1} are ascribed to the characteristic absorbance of $–CF_3$ and $–CF_2$, respectively. Disappearance of the characteristic peak of epoxy group at 914 cm^{-1} indicated the completion of the reaction between epoxy group and carboxyl acid group.

The ^1H NMR spectra of UVPA oligomer and PHFBMA-GMA-1/6 in $CDCl_3$ solvent are shown in Figures 3 and 4, respectively. In Figure 3, the characteristic resonance signals of the double-bond protons in 6.14 ppm and 5.59 ppm were detected. The resonance signals at 4.22 ppm belong to the protons of methane

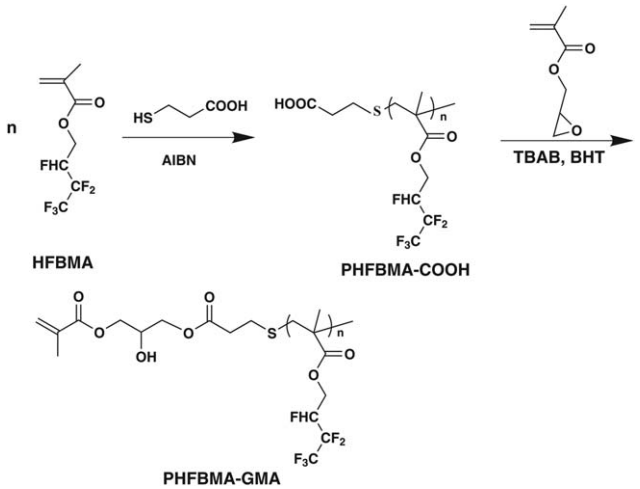

Scheme 2. Synthetic route of PHFBMA-GMA.

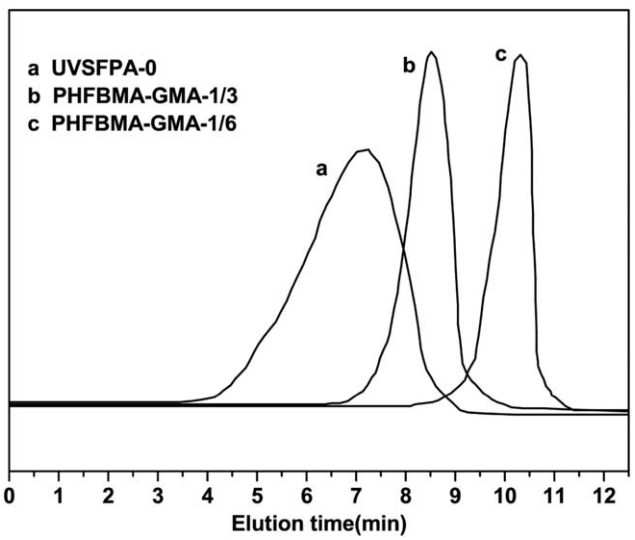

Figure 1. GPC curves of UVPA oligomer, PHFBMA-GMA-1/3, and PHFBMA-GMA-1/6.

Table IV. Surface Composition of UVSFPA-6, UVLFPA-1/3-6, and UVLFPA-1/6-6 Films Measured by XPS

	Theoretical atomic content (or bulk atomic content)/%			Experimental atomic content/%		
Sample	C	O	F	C	O	F
UVSFPA-6	71.66	26.70	1.64	70.40	27.91	1.69
UVLFPA-1/3-6	71.66	26.70	1.64	62.27	19.29	18.45
UVLFPA-1/6-6	71.66	26.70	1.64	64.03	22.88	13.10

-C***H***(OH)-(d). The signals at 4.03 ppm were ascribed to the methylene protons of e and h; Peaks at 3.50–3.71 ppm are ascribed to the methyl protons of i. The chemical shift ranging from 0.75–2.45 ppm represented the methylene protons of f, g, and methyl protons of c, respectively.

In Figure 4, the characteristic peaks at 6.14 ppm and 5.63 ppm represented the protons of the double bond in methacryloyloxy –C***H***$_2$=C(CH$_3$)- (a, b); signals at 4.78–5.18 ppm are designated to the splitting of -CHF(k); The chemical shift of 4.23–4.58 ppm belongs to the methylene protons of d, e, and j. The peaks at 2.60–2.80 ppm represent the methylene protons of f and g. The signals of 2.16–1.81 ppm and 1.67–0.81 ppm are assigned to the protons of h and c, i, respectively.

Surface Properties of UV-Cured Films

Surface properties of UV-cured films were characterized by contact angle and surface energy calculated from Owens and Wendt's method.[23] The data of contact angle and surface energy are summarized in Figures 5, 6, and 7, respectively. As can be seen, the water contact angle and surface energy of UVPA was 83.5°and 36.70 mN/m, respectively. Small amount of the PHFBMA-GMA is effective to create hydrophobic surface. Hydrophobic surface with surface energy of 28.17 mN/m could be obtained by just adding a small amount of reactive PHFBMA-GMA-1/3 (2 wt %) into the UV-cured films. The water contact angle of the resulting UV-cured films increased with increasing the concentration of PHFBMA-GMA added. Water contact angle increased much more slightly when the concentration of PHFBMA-GMA reached 6 wt %, the water contact angle was almost the same with the pure PHFBMA (102.6°), which suggesting that the surface energy was very close to the lower limit. Similar phenomenon could be observed in diiodomethane contact angles on the UV-cured films. It is because more fluorinated moieties migrate to the surface with increasing the concentration of PHFBMA-GMA. When the content of PHFBMA-GMA reached 6 wt % or more, the surface was saturated and the surface energy reached the minimum value.

It was found that, for a given content of the macromonomer, higher molecular weight led to higher contact angle and lower surface energy. Especially, the difference between UVSFPA and UVLFPA was extremely large. This may result from the poorer compatibility of higher molecular weight PHFBMA-GMA with PA. Longer fluorinated side chains have stronger thermodynamic driving force to migrate to the outermost layer, resulting in more fluorine atoms concentrated on the surface. While short fluorinated moieties were buried in the bulk of the polymer and difficult to migrate to the surface because of the restriction of the polymer backbone.[11] PHFBMA-GMA is a much more efficient and effective additive to generate hydrophobic surface.

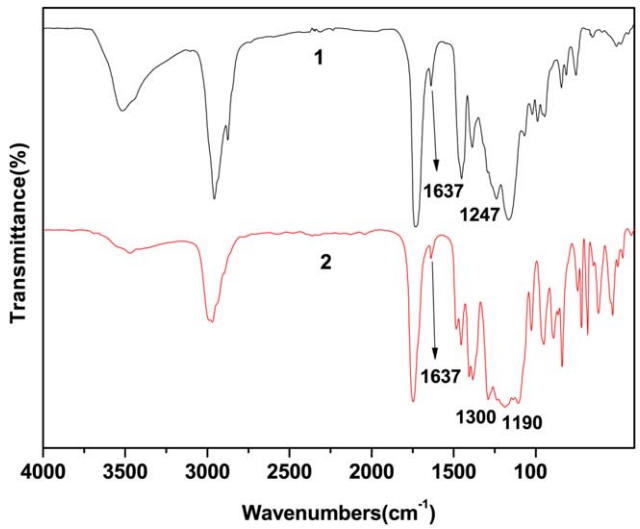

Figure 2. FTIR spectra of UVPA oligomer(trace 1) and PHFBMA-GMA-1/6 (trace 2). [Color figure can be viewed in the online issue, which is available at wileyonlinelibrary.com.]

Surface Composition of UV-Cured Films

XPS was employed to provide quantitative and qualitative analysis on the surface composition of the surface. Figure 8 showed

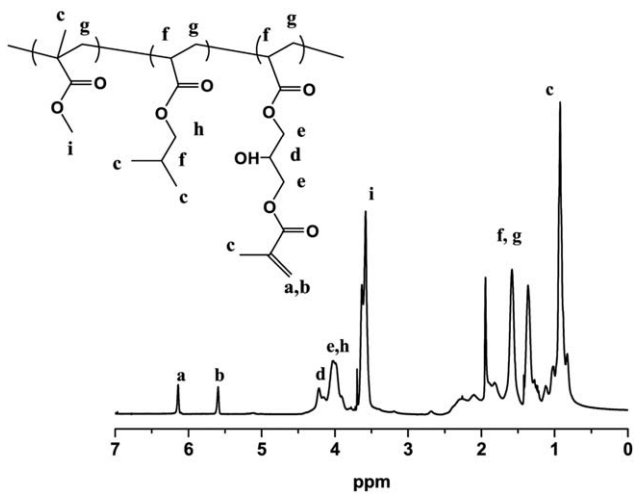

Figure 3. ^{1}H NMR spectra of UVPA oligomer.

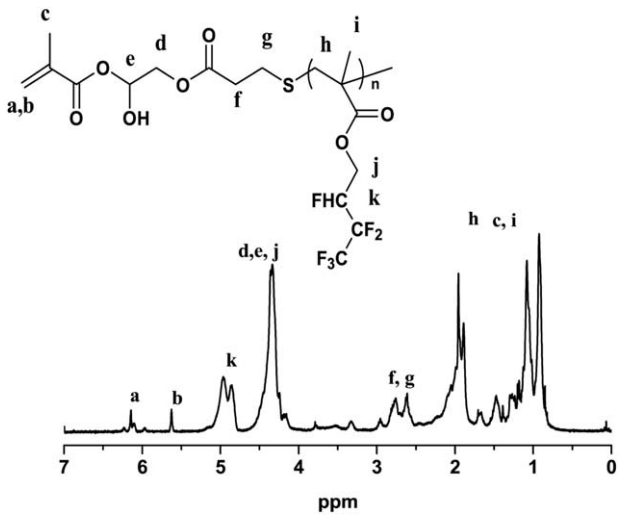

Figure 4. ^{1}H NMR spectra of PHFBMA-GMA-1/6.

the broad scan of the binding energy (BE) spectrum for UVLFPA-1/3-6 and UVLFPA-1/6-6 and UVSFPA-6, respectively. The peaks at 282.8, 530.9, and 686.6 eV are attributed to C1s, O1s, and F1s, respectively. As can be seen, the strong peak at 686.6 eV assigned to the fluorine atoms of UVLFPA-1/3-6 and UVLFPA-1/6-6 was much larger than that of UVSFPA-6, indicating more fluorine atoms concentrated on the surface of UVLFPA than UVSFPA. The surface composition data of UVLFPA-1/3-6, UVLFPA-1/6-6 and UVSFPA-6 are listed in Table IV.

The experimental fluorine atomic content (1.69%) of UVSFPA-6 at the surface was quite similar with the theoretical one (1.64%), indicating that few fluorine atoms migrate to the outmost layer. However, higher fluorine content was observed on the surface in longer fluorinated macromonomer chains. As can be seen, fluorine atomic content of UVLFPA-1/3-6 is slightly higher than UVLFPA-1/6-6. Especially, the fluorine atomic content of UVLFPA-1/3-6 (18.45% fluorine atomic content) and

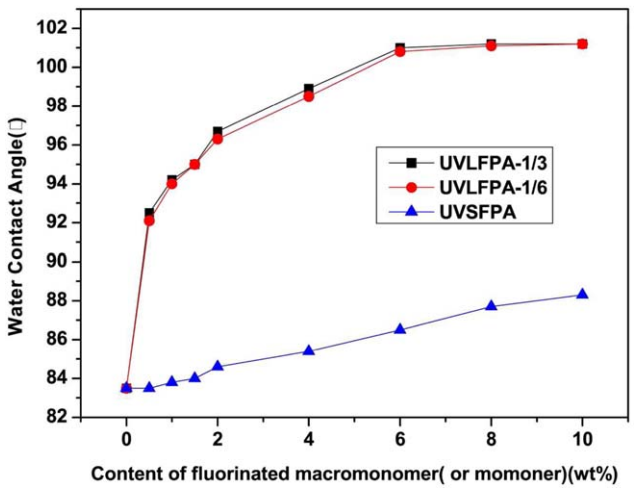

Figure 5. Water contact angle of UVLFPA and UVSFPA. [Color figure can be viewed in the online issue, which is available at wileyonlinelibrary.com.]

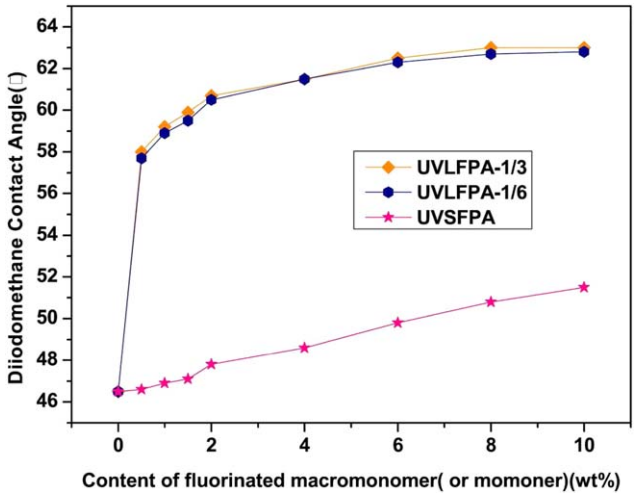

Figure 6. Diiodomethane contact angle of UVLFPA and UVSFPA. [Color figure can be viewed in the online issue, which is available at wileyonlinelibrary.com.]

UVLFPA-1/6-6 (13.10% fluorine atomic content) was far higher than that of UVSFPA-6 (1.69% fluorine atomic content), even though their fluorine content in bulk is the same. These results were well consistent with the contact angle measurement. Data from XPS analysis was a strong evidence confirming the fact that long fluorinated side chains, which have greater thermodynamic driving force to migrate to the surface due to the incompatibility with the matrix, are more efficient and effective to migrate and concentrate on the surface than short pendent fluorinated group.[8,30,31]

Gel Content and Water Absorption of UV-Cured Films

Gel content tests were employed to measure the curing and crosslink degree of the UV-cured films. Gel content results are summarized in Table V. Gel content of all the UV-cured films exceeded 90%, which indicated outstanding curing and crosslink degree for the films.

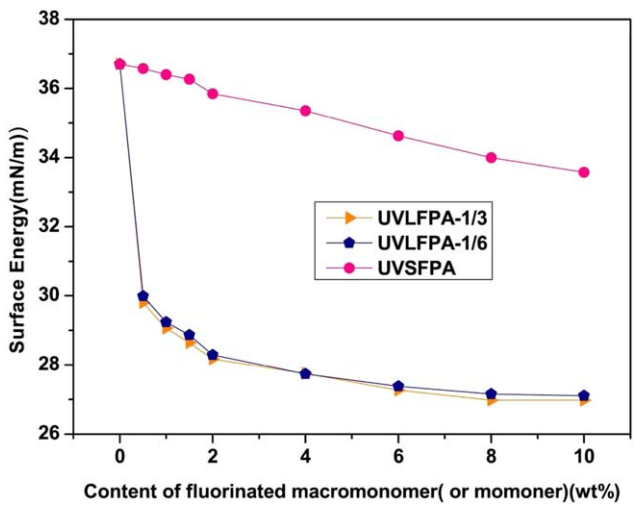

Figure 7. Surface energy of UVLFPA and UVSFPA. [Color figure can be viewed in the online issue, which is available at wileyonlinelibrary.com.]

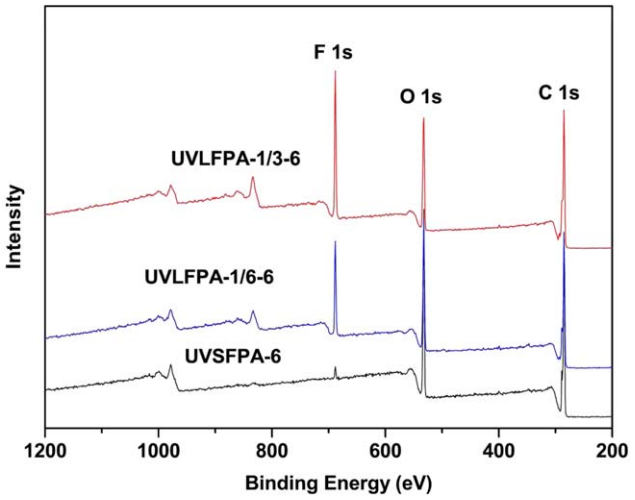

Figure 8. XPS curves of UVSFPA-6, UVLFPA-1/3-6, and UVLFPA-1/6-6 films. [Color figure can be viewed in the online issue, which is available at wileyonlinelibrary.com.]

Pencil Hardness and Adhesion of UV-Cured Films

Hardness and adhesion are two significant parameters for evaluating the properties of coatings. Pencil hardness and adhesion test results are summarized in Table V. Pencil hardness of all the samples was in the range of H–2H. This was attributed to the suitable collocation between hard monomers and soft monomers in the polymer backbone. Most importantly, in the micro scale, the three-dimensional cross-linking network structures formed during the UV cure process strongly restricted the motion of the polymer segments. Thus, hard coating was performed in the macro scale. When the amount of PHFBMA-GMA exceeded 8 wt %, the pencil hardness reduced to level H. This might be attributed to lower cross-linking density with increasing the amount of PHFBMA-GMA, since the content of C=C of PHFBMA-GMA was lower than that of UVPA oligomer under the same weight.

Conventionally, the fluorinated coatings somewhat exhibit poor adhesion due to the fluorinated moieties have different solubility parameter from most materials.[32] In our work, PHFBMA-GMA added in the UV coatings did not deteriorate the adhesion. UVLFPA films showed extremely excellent adhesion (5B) on the substrates (PC, PET, and PMMA). This is probably attributed to two main reasons: On one hand, the chemical structures such as the polar ester groups bearing in the coating had good affinity with the substrate. On the other hand, the fluorinated moieties migrated to the surface along with the long fluorinated chains and kept far from the interface between the coating and the substrate and did not affect the interaction between the polymer and the substrate.[33,34]

Chemical Resistance of UVLFPA

Chemical resistance of UV-cured coatings was investigated in terms of the absorption percentage of the UV-cured films in 10 wt % HCl and 10 wt % NaOH. The results are summarized in Table VI. All the films were not destroyed into fragments and the appearance of the films remained no change except in NaOH. Furthermore, absorption in NaOH was higher than that in HCl, indicating less tolerance in alkaline environment. That might be because the ester groups of the polymer were not as tolerant in alkaline as in acidic conditions. In addition, the absorption of the modified films was lower than the one without fluorinated macromonomer or monomer. Absorption decreased with increasing the content of PHFBMA-GMA. This test revealed that the resistance of coatings to different type of chemicals was quite excellent.

Mechanical Properties of UVLFPA

Mechanical properties, including tensile strength and modulus, are summarized in Figure 9. As can be seen, the tensile strength of UVLFPA, ranging from 7.55 to 13.60 MPa, increased at first then decreased with further increasing the content of PHFBMA-GMA. The maximum value of modulus was observed when the content of the fluorinated macromonomer was 6 wt %. There are two competitive factors that affect the mechanical properties. On one hand, the hard segments of PHFBMA-GMA contributed to the enhancement of the strength of the UV-cured films. While with increasing the content of PHFBMA-GMA, the cross-linking density decreased since the content of C=C of

Table V. Gel Content, Water Absorption, Pencil Hardness, and Adhesion of UV-Cured Films

				Adhesion		
Samples	Gel content (%)	Water absorption (%)	Pencil hardness	on PC	on PET	on PMMA
UVPA	95	1.61	H	5B	5B	5B
UVLFPA-1/3-2	96	1.36	H	5B	5B	5B
UVLFPA-1/3-4	98	1.23	2H	5B	5B	5B
UVLFPA-1/3-6	97	1.15	2H	5B	5B	5B
UVLFPA-1/3-8	95	0.71	H	5B	5B	5B
UVLFPA-1/3-10	92	0.60	H	5B	5B	5B
UVLFPA-1/6-2	95	1.42	H	5B	5B	5B
UVLFPA-1/6-4	97	1.28	2H	5B	5B	5B
UVLFPA-1/6-6	98	1.15	2H	5B	5B	5B
UVLFPA-1/6-8	93	0.64	H	5B	5B	5B
UVLFPA-1/6-10	93	0.63	H	5B	5B	5B

Table VI. Chemical Resistance of UV-Cured Films

	HCl (10 wt %)		NaOH (10 wt %)	
Samples	Appearance	Absorption (%)	Appearance	Absorption (%)
UVPA	No change	1.61	Yellowish	2.21
UVLFPA-1/3-2	No change	1.36	Yellowish	1.86
UVLFPA-1/3-4	No change	1.23	Yellowish	1.80
UVLFPA-1/3-6	No change	1.15	Yellowish	1.69
UVLFPA-1/3-8	No change	0.71	Yellowish	1.66
UVLFPA-1/3-10	No change	0.60	Yellowish	1.58
UVLFPA-1/6-2	No change	1.42	Yellowish	1.79
UVLFPA-1/6-4	No change	1.28	Yellowish	1.68
UVLFPA-1/6-6	No change	1.15	Yellowish	1.60
UVLFPA-1/6-8	No change	0.64	Yellowish	1.55
UVLFPA-1/6-10	No change	0.63	Yellowish	1.54

PHFBMA-GMA was lower than that of UVPA oligomer under the same weight. The tensile strength and the modulus of the UV-cured films were combined results of these two competitive factors. Overall, the tensile strength and the modulus of UVLFPA-1/6 were higher than that of UVLFPA-1/3 probably due to the higher cross-linking density. It is noteworthy that the tensile strength of all the UV-cured films modified with the fluorinated macromonomer was higher than that of films without fluorinated macromonomer or monomer.

Optical Transmittance of UVLFPA

Phase separation may occur when fluorinated macromonomer was blended with the polymer matrix since fluoropolymers are incompatible with most other materials in most cases. As a result, the UV-cured films may be heterogeneous and opaque and can be hardly applied in the fields requiring high transparency. The optical transmittance of the UVWAGC was measured by UV–vis spectrometer and the results are shown in Figure 10. The transmittance of all samples containing PHFBMA-GMA were above 90% and even reached 100% in the range of visible wavelength (400–800 nm), which were quite similar with the neat UVPA films except for UVLFPA-1/3-8 (88% at 400 nm) which might have the largest aggregates formed by fluorinated moieties. In the present work, the reactive surface modifier added into UVPA did not affect the transparency of the UV-cured films.

Thermal Properties of UVLFPA

DSC and thermo gravimetric analysis (TGA) were employed to characterize the thermal properties of UVLFPA. DSC thermograms of the UVLFPA samples and the T_g values are summarized in Figure 11 and Table VII, respectively. The results showed that only one T_g transition was observed, indicating that no phase separation occurred. There were three main factors affecting the mobility of the UV-cured films: Firstly, MMA are hard monomers and they hindered the motion of the segments; secondly, the long fluorinated side chains intensified the entanglement among the polymer chains; thirdly, in the microscale, three-dimensional cross-linking network structure among the polymers was formed during the UV process. All these three factors hindered the mobility of the segments. The T_g values of

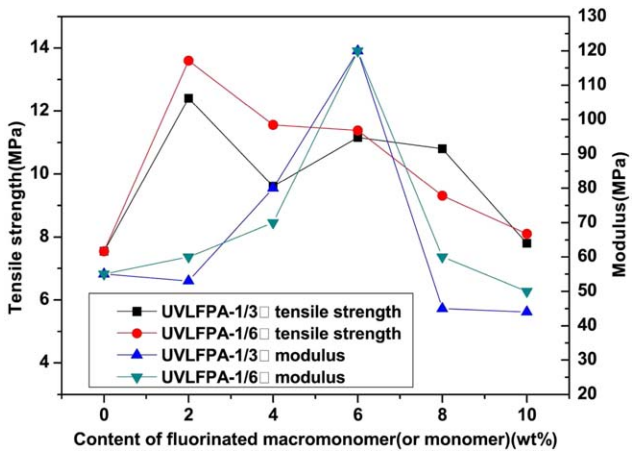

Figure 9. Tensile strength and modulus of UVLFPA-1/3 and UVLFPA-1/6. [Color figure can be viewed in the online issue, which is available at wileyonlinelibrary.com.]

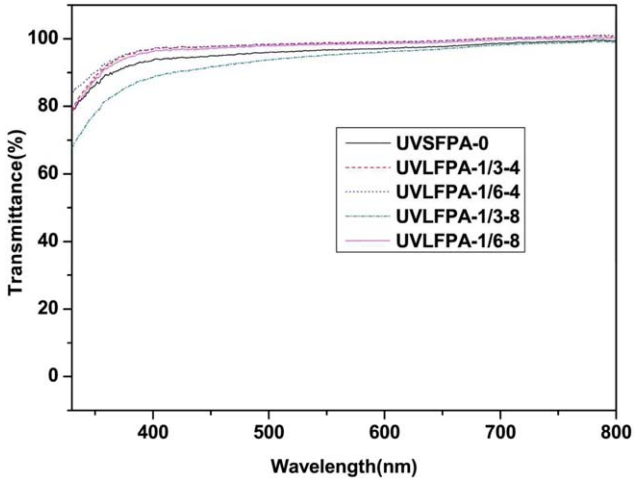

Figure 10. Optical transmittance spectrums of UVLFPA. [Color figure can be viewed in the online issue, which is available at wileyonlinelibrary.com.]

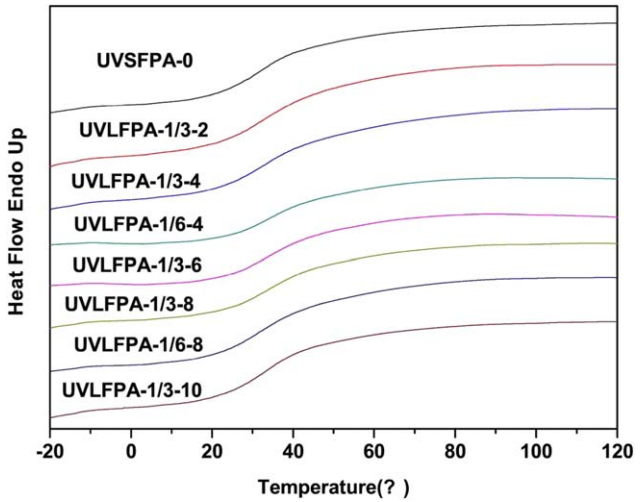

Figure 11. DSC thermograms of UVLFPA. [Color figure can be viewed in the online issue, which is available at wileyonlinelibrary.com.]

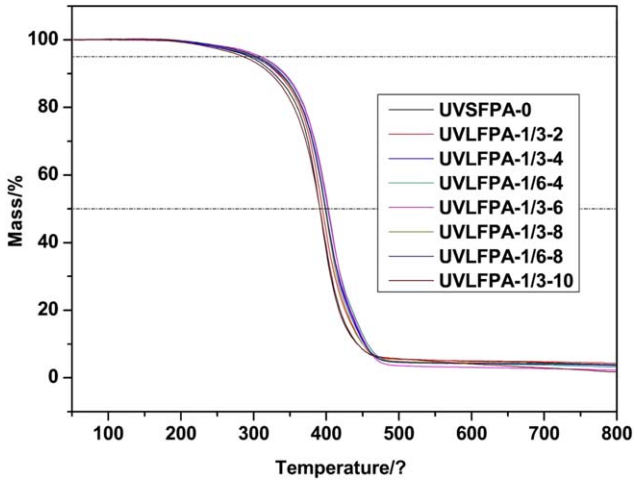

Figure 12. TGA thermograms of UVLFPA. [Color figure can be viewed in the online issue, which is available at wileyonlinelibrary.com.]

the UV-cured films increased firstly with increasing the amount of PHFBMA-GMA. This might be attributed to the intensified the entanglement of long fluorinated chains. However, T_g decreased slightly when the amount of macromonomer exceeded 8 wt %. This can be explained that with increasing the amount of PHFBMA-GMA, the cross-linking density of the UV-cured films decreased, thus the mobility of the UV-cured films was intensified, since the macromonomer had lower C=C functionalities than UVPA oligomer under the same weight.

TGA and DTG curves and the thermal parameters including initial degradation temperature at weight loss of 5, 50 wt % ($T_{d5\%}$, $T_{d50\%}$), the maximum rate of weight loss (T_{max}) decomposition temperatures are summarized in Figures (12 and 13), and Table VII, respectively. All samples showed excellent thermal properties. This is attributed to two main reasons: On one hand, the chemical bonding energy of C–F is extremely high (540 kJ/mol) and the fluorinated polymers have outstanding thermal stability;[35,36] on the other hand, three-dimensional cross-linking structure was formed after UV cured, thus the thermal stability of the films was improved. With increasing the content of PHFBMA-GMA, the thermal parameters of the UV-cured films increased first then decreased slightly. This can be explained that the cross-linking density of the UV-cured films decreased with increasing the amount of PHFBMA-GMA since the macromonomer had lower C=C functionalities than UVPA oligomer under the same weight. As can be seen, $T_{5\%}$, $T_{50\%}$, and T_{max} of UVWAGC films were far higher than pure UVWAC films. As a result, introduction of the long fluorinated side chains into the polymer decelerated the thermal decomposition and improved the thermal stability of the films.

Table VII. Thermal Properties of UV-Cured Films

Samples	T_g (°C)	$T_{5\%}$ (°C)	$T_{50\%}$ (°C)	T_{max} (°C)
UVPA	31.04	295.5	390.9	394.4
UVLFPA-1/3-2	32.27	299.8	395.1	395.7
UVLFPA-1/3-4	33.24	299.4	399.5	400.4
UVLFPA-1/6-4	32.84	309.8	402.1	402.9
UVLFPA-1/3-6	34.59	310.0	402.9	406.2
UVLFPA-1/3-8	35.02	301.3	397.9	400.4
UVLFPA-1/6-8	34.89	305.6	399.2	400.4
UVLFPA-1/3-10	33.12	286.2	390.9	396.3

CONCLUSION

A novel mono-methacryloyloxy terminated fluorinated macromonomer (PHFBMA-GMA) was successfully synthesized and characterized. Then, PHFBMA-GMA was used as a reactive modified additive to modify the UV-cured polyacrylate. Contact angle measurement showed that a small amount of PHFBMA-GMA added to UVPA could generate hydrophobic surface. Surface energy of UVLFPA decreased with increasing both the content and the molecular weight of PHFBMA-GMA. XPS showed that fluorine atomic content of UVLFPA was much larger than that of UVSFPA, confirming the enrichment of fluorine atoms on the surface of UVLFPA. The UV-cured films performed

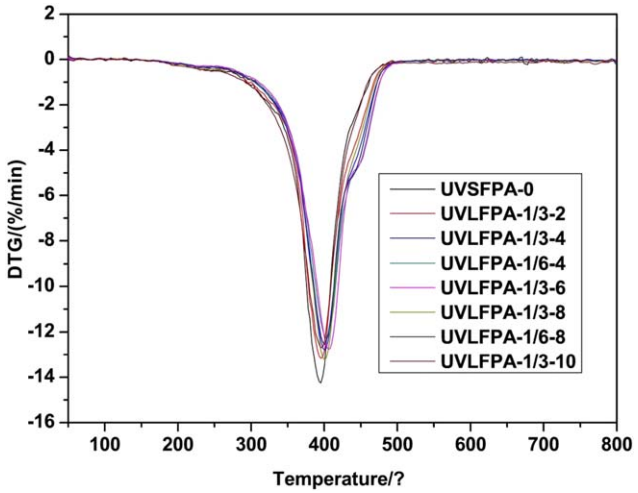

Figure 13. DTG thermograms of UVLFPA. [Color figure can be viewed in the online issue, which is available at wileyonlinelibrary.com.]

pencil hardness ranging from H to 2H. In addition, PHFBMA did not affect the adhesion and transparency and the UV-cured films maintained 5B adhesion and 90% or more transmittance. Moreover, the thermal properties of the UVLFPA were improved.

ACKNOWLEDGMENTS

This study was supported by the Key Laboratory of Cellulose and Lignocellulosics, Guangzhou Institute of Chemistry, Chinese Academy of Sciences, and the Natural Science Foundation of Guangdong Province (No. S2013010012106).

REFERENCES

1. Rengasamy, S.; Mannari, V. *Prog. Org. Coat.* **2013**, *76*, 78.
2. Chattopadhyay, D. K.; Panda, S. S.; Raju, K. *Prog. Org. Coat.* **2005**, *54*, 10.
3. Ciardelli, F.; Aglietto, M.; di Mirabello, L. M.; Passaglia, E.; Giancristoforo, S.; Castelvetro, V.; Ruggeri, G. *Prog. Org. Coat.* **1997**, *32*, 43.
4. Saïdi, S.; Guittard, F.; Guimon, C.; Géribaldi, S. *Macromol. Chem. Phys.* **2005**, *206*, 1098.
5. Saidi, S.; Guittard, F.; Guimon, C.; Géribaldi, S. *J. Polym. Sci. Pol. Chem.* **2005**, *43*, 3737.
6. Miao, H.; Bao, F.; Cheng, L.; Shi, W. *J. Fluorine. Chem.* **2010**, *131*, 1356.
7. Miao, H.; Cheng, L.; Shi, W. *Prog. Org. Coat.* **2009**, *65*, 71.
8. Yan, Z.; Liu, W.; Gao, N.; Ma, Z.; Han, M. *J. Fluorine Chem.* **2013**, *147*, 49.
9. Malshe, V. C.; Sangaj, N. S. *Prog. Org. Coat.* **2005**, *53*, 207.
10. Malshe, V. C.; Elango, S.; Bhagwat, S. S.; Maghrabi, S. S. *Prog. Org. Coat.* **2005**, *53*, 212.
11. Li, K.; Wu, P.; Han, Z. *Polymer* **2002**, *43*, 4079.
12. Park, I. J.; Lee, S. B.; Choi, C. K. *Macromolecules* **1998**, *31*, 7555.
13. Wang, J.; Mao, G.; Ober, C. K.; Kramer, E. J. *Macromolecules* **1997**, *30*, 1906.
14. Wang, J.; Ober, C. K. *Macromolecules* **1997**, *30*, 7560.
15. Park, I. J.; Lee, S. B.; Choi, C. K. *Polymer* **1997**, *38*, 2523.
16. Sun, Y.; Liu, W. *J. Polym. Res.* **2012**, *19*, 1.
17. Ameduri, B.; Bongiovanni, R.; Lombardi, V.; Pollicino, A.; Priola, A.; Recca, A. *J. Polym. Sci. Pol. Chem.* **2001**, *39*, 4227.
18. Yildiz, U.; Hazer, B.; Tauer, K. T. *Polym. Chem.* **2012**, *3*, 1107.
19. Hazer, B. *Die Makromol. Chem.* **1992**, *193*, 1081.
20. Ito, K. *Prog. Polym. Sci.* **1998**, *23*, 581.
21. Keleş, E.; Hazer, B.; Cömert, F. B. *Mater. Sci. Eng. C Mater.* **2013**, *33*, 1061.
22. Hazer, B. *Polym. Degr. Stab.* **2015**, *119*, 159.
23. Owens, D. K.; Wendt, R. C. *J. Appl. Polym. Sci.* **1969**, *13*, 1741.
24. Chen, G. F.; Jones, F. N. *Macromolecules* **1991**, *24*, 2151.
25. Teodorescu, M.; Dimonie, M.; Cerchez, I. *Eur. Polym. J.* **1999**, *35*, 247.
26. Teodorescu, M. *Eur. Polym. J.* **2002**, *38*, 841.
27. Miyauchi, N.; Kirikihira, I.; Li, X.; Akashi, M. *J. Polym. Sci. Pol. Chem.* **1988**, *26*, 1561.
28. Akashi, M.; Kirikihira, I.; Miyauchi, N. *Die Angew. Makromol. Chem.* **1985**, *132*, 81.
29. Akashi, M.; Yamashita, I.; Miyauchi, N. *Die Angew. Makromol. Chem.* **1984**, *122*, 147.
30. Lin, Y. H.; Liao, K. H.; Huang, C. K.; Chou, N. K.; Wang, S. S.; Chu, S. H.; Hsieh, K. H. *Polym. Int.* **2010**, *59*, 1205.
31. Van de Grampel, R. D.; Ming, W.; Van Gennip, W. J. H.; Van der Velden, F.; Laven, J.; Niemantsverdriet, J. W.; Van der Linde, R. *Polymer* **2005**, *46*, 10531.
32. Bongiovanni, R.; Di Gianni, A.; Priola, A.; Pollicino, A. *Eur. Polym. J.* **2007**, *43*, 3787.
33. Bongiovanni, R.; Medici, A.; Zompatori, A.; Garavaglia, S.; Tonelli, C. *Polym. Int.* **2012**, *61*, 65.
34. Sangermano, M.; Di Gianni, A.; Bongiovanni, R.; Priola, A.; Voit, B.; Pospiech, D.; Appelhans, D. *Macromol. Mater. Eng.* **2005**, *290*, 721.
35. Tang, C.; Liu, W.; Ma, S.; Wang, Z.; Hu, C. *Prog. Org. Coat.* **2010**, *69*, 359.
36. Jariwala, C. P.; Mathias, L. J. *Macromolecules* **1993**, *26*, 5129.